ChemPubSoc Europe

DOI: 10.1002/cssc.201902347

CHEMSUSCHEM Communications

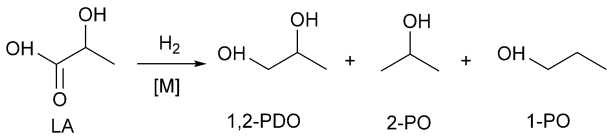
$Mg(OH)_2$-Facilitated Liquid-Phase Conversion of Lactic Acid into 1,2-Propanediol over Cu: An Experimental and Theoretical Study

Xinde Wang, Anna Katharina Beine, Peter J. C. Hausoul, and Regina Palkovits*[a]

$Mg(OH)_2$ is found to exhibit superior performance in the liquid-phase conversion of lactic acid (LA) into 1,2-propanediol over Cu. A conversion of 90% with a selectivity of 98% is achieved at 513 K and 5 MPa H_2. $Mg(LA)_2$ could be identified as a crucial intermediate in this reaction, as it undergoes faster conversion than the combination of LA and $Mg(OH_2)$ and regeneration of $Mg(OH)_2$ through the conversion of $Mg(LA)_2$ as a substrate. DFT calculations reveal that the energetic span of the reaction decreases from 46.6 kcal mol^{-1} catalyzed with no cation to 43.6 kcal mol^{-1} with $[Mg(OH)]^+$, confirming the facilitating effect of $Mg(OH)_2$.

Lactic acid (LA) has attracted increasing attention, owing to its use as monomer for biodegradable polylactic acid (PLA).[1] Consequently the production of L-lactic acid, a naturally occurring organic acid, by bacterial fermentation of carbohydrates has been steadily rising.[2] Although relatively selective, still significant amounts of the other enantiomers (e.g., D-lactic acid) are produced, causing extra expense for separation for the production of PLA. LA is also produced as an unavoidable side product in the hydrogenolysis of biomass to glycols.[3] However, in this case LA is racemic and generally unsuitable for the production of PLA. Hence routes for the conversion of LA into value-added products are important when considering its large-scale production.[4] Particularly, the direct conversion of biogenic LA into 1,2-propanediol (1,2-PDO) in the liquid phase is attractive, given the potential for CO_2 reduction and the wide application of 1,2-PDO as a monomer and as a constituent in antifreezes (Scheme 1).[5]

Hydrogenation of LA was initially reported by Broadbent and Whittle, who obtained a yield of 84% at 423 K and 26 MPa H_2 using a Re-black catalyst.[6] Zhang et al. investigated multiple catalysts and observed superior activity for Ru/C.[7] A conversion of 95% with 90% selectivity to 1,2-PDO was obtained at 423 K and 14.5 MPa H_2. Furthermore, Takeda et al. improved



Scheme 1. Metal-catalyzed hydrogenolysis of LA to 1,2-PDO and alcohols.

the catalytic performance of Ru/C by doping with MoO_x species, which led to a yield of 95% at 393 K and 8 MPa H_2.[8] Besides highly active Ru catalysts, non-noble metals have also been investigated.[9] Cortright et al. reported full conversion with a selectivity of 88% to 1,2-PDO over Cu/SiO_2 at 473 K in the gas phase.[9g] The authors proposed a two-step reaction mechanism involving dehydration over the SiO_2 support and hydrogenation over Cu. Notably, in the liquid phase reaction no conversion of LA was observed. However, in our previous study on the hydrogenolysis of sorbitol in water we observed that conversion of LA into 1,2-PDO leads to increasing glycol selectivity.[10] Herein we present the direct conversion of LA under basic conditions by using SiO_2-supported Cu catalysts. The influence of the added base on the course of the reaction and the reaction mechanism was studied in detail. DFT calculations were performed and suggest a strong influence of the cation on the reaction mechanism.

The Cu/SiO_2 catalyst was prepared by using the ammonia evaporation precipitation method. The metal loading was determined by inductively coupled plasma optical emission spectroscopy (ICP-OES) to be 24.2 wt%. N_2 physisorption revealed that Cu/SiO_2 had a surface area of 279 $m^2 g^{-1}$ and a pore volume of 0.71 $cm^3 g^{-1}$. The addition of Cu did not modify the surface area (287 $m^2 g^{-1}$) or pore volume (0.88 $cm^3 g^{-1}$) of SiO_2 significantly. The adsorption and desorption isotherms are shown in Figure S1 (see the Supporting Information). The particle distribution was investigated by using TEM (Figure 1). The Cu particle size is 13.1 ± 3.6 nm.

[a] X. Wang, Dr. A. K. Beine, Dr. P. J. C. Hausoul, Prof. Dr. R. Palkovits
Institut für Technische und Makromolekulare Chemie
RWTH Aachen University, Worringerweg 2, 52074 Aachen (Germany)
E-mail: palkovits@itmc.rwth-aachen.de

Supporting Information and the ORCID identification number(s) for the author(s) of this article can be found under: https://doi.org/10.1002/cssc.201902347.

© 2019 The Authors. Published by Wiley-VCH Verlag GmbH & Co. KGaA. This is an open access article under the terms of the Creative Commons Attribution License, which permits use, distribution and reproduction in any medium, provided the original work is properly cited.

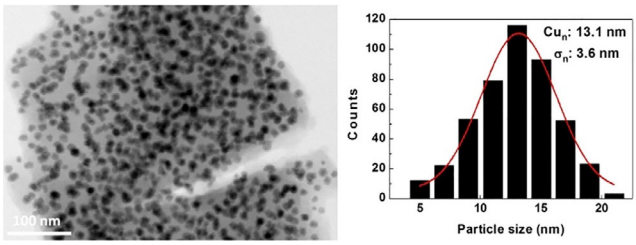


Figure 1. TEM image and particle size distribution of Cu/SiO_2.

 © 2020 The Authors. Published by Wiley-VCH Verlag GmbH & Co. KGaA, Weinheim

The influence of temperature on the conversion was investigated in the presence of $Mg(OH)_2$ at 5 MPa H_2 (Figure 2a). High selectivities of up to 98% were achieved in all cases, indicating that Cu is an excellent catalyst to produce 1,2-PDO. The

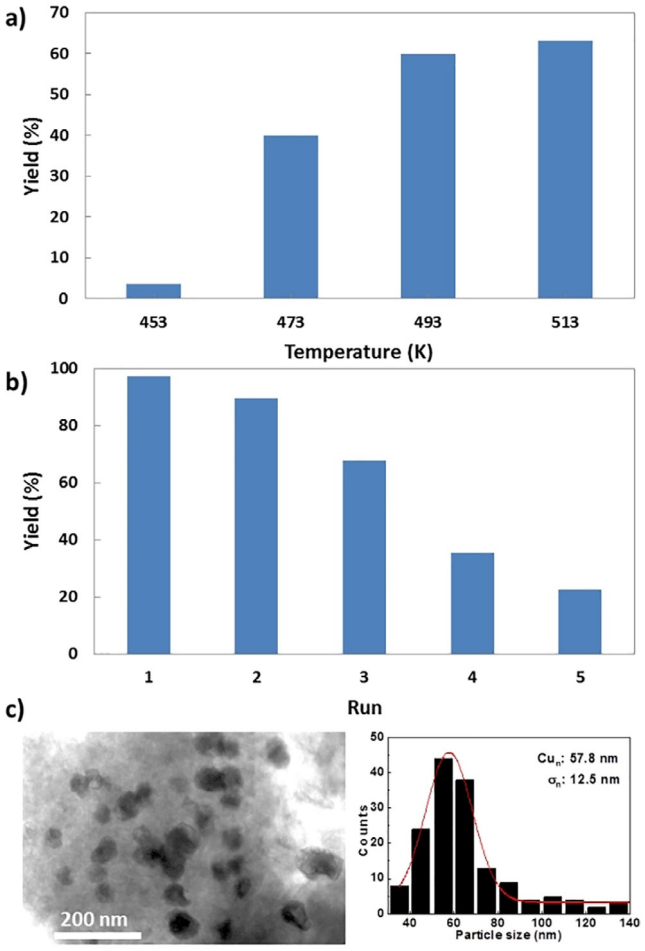


Figure 2. a) Temperature dependence of LA conversion over 25% wt% Cu/SiO_2. Reaction conditions: catalyst (0.1 g), LA (0.5 g), $Mg(OH)_2$ (0.4 g), H_2O (20 mL), H_2 (5 MPa), 4 h. b) Recycling of 25% Cu/SiO_2 over five runs. Reaction conditions: 25% Cu/SiO_2 (0.1 g), $Mg(LA)_2$ (0.56 g), H_2O (20 mL), 513 K, H_2 ()5 MPa, 4 h. c) TEM image and particle distribution of the five-times-recycled 25% Cu/SiO_2 catalyst.

conversion increases from 4% at 453 K to 63% at 513 K. Notably, a conversion of 40% was obtained at 473 K, confirming that Cu can also be employed at lower temperatures. The increased reaction rate is partially attributed to the higher solubility of $Mg(OH)_2$ at the higher temperature, favoring the generation of $Mg(LA)_2$. Furthermore, the influence of the H_2 pressure on the reaction rate was investigated (Figure S2). At 513 K, the conversion increased from 16% at 1 MPa to 86% at 4 MPa, although further increase in the H_2 pressure did not lead to higher conversion. The pressure dependence below 4 MPa is attributed to mass transfer limitations, owing to the three-phase reaction. To exclude this effect, all reactions were carried out at 5 MPa H_2. To test the long-term catalyst stability, five consecutive recycling experiments were carried out using 25 wt% Cu/SiO_2 (Figure 2b). Conversion continuously decreased from 97% in the first run to 23% in the fifth run. ICP-OES of the reaction solution showed only minimal Cu leaching ($\leq$0.1%; Table S1). TEM of the spent catalyst revealed a significant agglomeration of the nanoparticles (Figure 2c). The Cu particle size increased from 13.1 nm for the fresh catalyst to 57.8 nm for the five-times-recycled one. This is in line with our previous observations on the conversion of sorbitol over Cu/AC, where the observed deactivation could be attributed to sintering of nanoparticles.[10] This once again demonstrates that further studies on the synthesis of stable Cu catalysts are necessary.

The influence of the type of base on the conversion of LA over Cu/SiO_2 is displayed in Figure 3a. In every experiment, the amount of OH^- in the reaction mixture was kept the same.

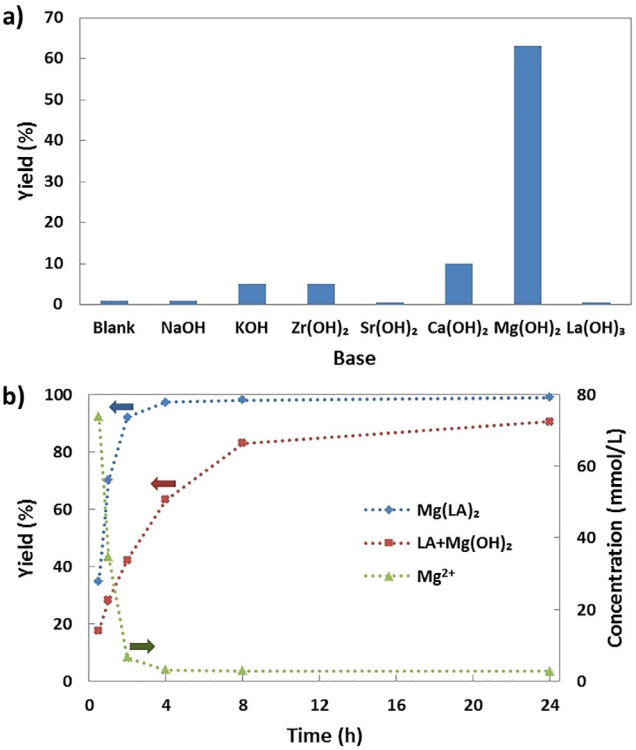


Figure 3. a) Influence of base on LA conversion over 25% Cu/SiO_2. Reaction conditions: 25% Cu/SiO_2 (0.1 g), LA (0.5 g), OH^- (68.5 mmol), H_2O (20 mL), 513 K, H_2 (5 MPa), 4 h. b) Conversion of $Mg(LA)_2$ and LA in the presence of $Mg(OH)_2$ over Cu/SiO_2 and the evolution of Mg^{2+} concentration over time. Reaction conditions: 25% Cu/SiO_2 (0.1 g), $Mg(LA)_2$ (0.56 g), LA (0.5 g), $Mg(OH)_2$ (0.4 g), H_2O (20 mL), 513 K, H_2 (5 MPa).

A reaction without base gave almost no conversion, indicating that Cu/SiO_2 alone is inactive, which is in accordance with the results reported by Cortright et al.[9g] The bases NaOH, $Sr(OH)_2$ and $La(OH)_3$ gave almost no conversion (<3%). KOH, $Zr(OH)_2$ and $Ca(OH)_2$ reached slightly higher conversion of up to 10%. However, with $Mg(OH)_2$ a significant increase in activity was achieved. 63% of LA was converted within 4 h and extending the reaction time to 24 h led to 90% conversion (Figure 3). When the reaction was carried out in the presence of $Mg(OH)_2$ but without Cu/SiO_2, conversion again did not exceed 3%. To

© 2020 The Authors. Published by Wiley-VCH Verlag GmbH & Co. KGaA, Weinheim

our knowledge, this is the first example of the conversion of LA into 1,2-PDO with promising yield over a Cu catalyst in the liquid phase. Increasing the equivalence of $Mg(OH)_2$ (see Figure S3) shows that the reaction is accelerated. This suggests that the dissolution of $Mg(OH)_2$ is rate-limiting. To test whether solid $Mg(OH)_2$ participates in the reaction, a test was performed with magnesium lactate ($Mg(LA)_2$), which is fully water-soluble. The time course of the reaction is displayed in Figure 3b. Compared to the reaction of LA in the presence of $Mg(OH)_2$, the conversion of $Mg(LA)_2$ proceeds much faster. A conversion of up to 92% was obtained in the first 2 h, whereas for LA + $Mg(OH)_2$ only 42% conversion was observed. Given the poor solubility of $Mg(OH)_2$, the greatly accelerated conversion can be attributed to the high solubility of $Mg(LA)_2$. The evolution of the Mg^{2+} concentration during the reaction was analyzed by ICP-OES. The concentration of Mg^{2+} decreased from 73.9 mmol L^{-1} at 0.5 h to 6.6 mmol L^{-1} at 2 h (Figure 3b). After the reaction, the pH of the solution was around 10, which is higher than would be expected from $Mg(LA)_2$ alone. Furthermore, the formation of a white powder that could be dissolved in HCl was observed after the reaction. This confirms that $Mg(OH)_2$ was generated during the reaction. These observations suggest that soluble Mg species play an important role in the conversion of LA facilitated by $Mg(OH)_2$.

To obtain deeper insights into the role of Mg^{2+} on the conversion of lactate to 1,2-PDO, DFT calculations at the B3LYP/6-311++G**/SMD(water) level of theory were carried out.[11] The proposed reaction mechanisms and their energy profiles are displayed in Figure 4 (see Figure S4 for the calculated geometries and Table S2 for obtained *d*G values). As both Cu and $Mg(OH)_2$ are necessary for the conversion, a synergistic reaction mechanism composed of a base/cation-catalyzed part and a Cu-catalyzed part is proposed. The OH^- catalyzed reaction sequence [i.e. with no cation (NC)] is considered as a benchmark. Preliminary calculations showed that dissolved $Mg(OH)_2$ is hydrated and in equilibrium with the cationic species $[Mg(OH)(H_2O)_5]^+$ and $[Mg(H_2O)_5]^{2+}$ and OH^-.[12] In the presence of LA, OH^- is neutralized, leading to the formation of LA^- and after coordination with Mg to $[Mg(OH)(LA)(H_2O)_2)]$ and $[Mg(LA)(H_2O)_3]^+$, respectively (**IM1**). Neutralization is strongly exothermic [−23.6 (NC), −27.2 ($[Mg(OH)]^+$) and −27.1 (Mg^{2+}) kcal mol^{-1}]. The lower *d*G of the magnesium lactate complexes suggests that magnesium cations have a high affinity for the lactate anion. Next, a proton transfer from the α-hydroxy group to the carboxylic group leads to **IM2** and activation of the α-carbon. In all cases proton transfer are endothermic, requiring 23.6 (NC), 15.3 ($[Mg(OH)(LA)(H_2O)_2]$) and 14.9 kcal mol^{-1} ($[Mg(LA)(H_2O)_3]^+$), respectively. For path NC, the proton is bridged between the hydroxy and carboxylic acid groups, whereas for the Mg-ion paths, the proton is fully shifted to the carboxylic acid. Compared to NC, binding with cation is highly beneficial and lowers the energy for proton transfer by 8 kcal mol^{-1}. Subsequently, a hydride shifts from the activated α-carbon to the carbonyl via transition state **TS1** and results in the formation of gem-diolate **IM3**. For this step, the Mg-ion paths exhibit higher barriers of 29.9 ($[Mg(OH)]^+$) and 28.3 (Mg^{2+}) kcal mol^{-1} as compared to 23.0 for NC. The hydride is approximately located over the middle of C–C bond.

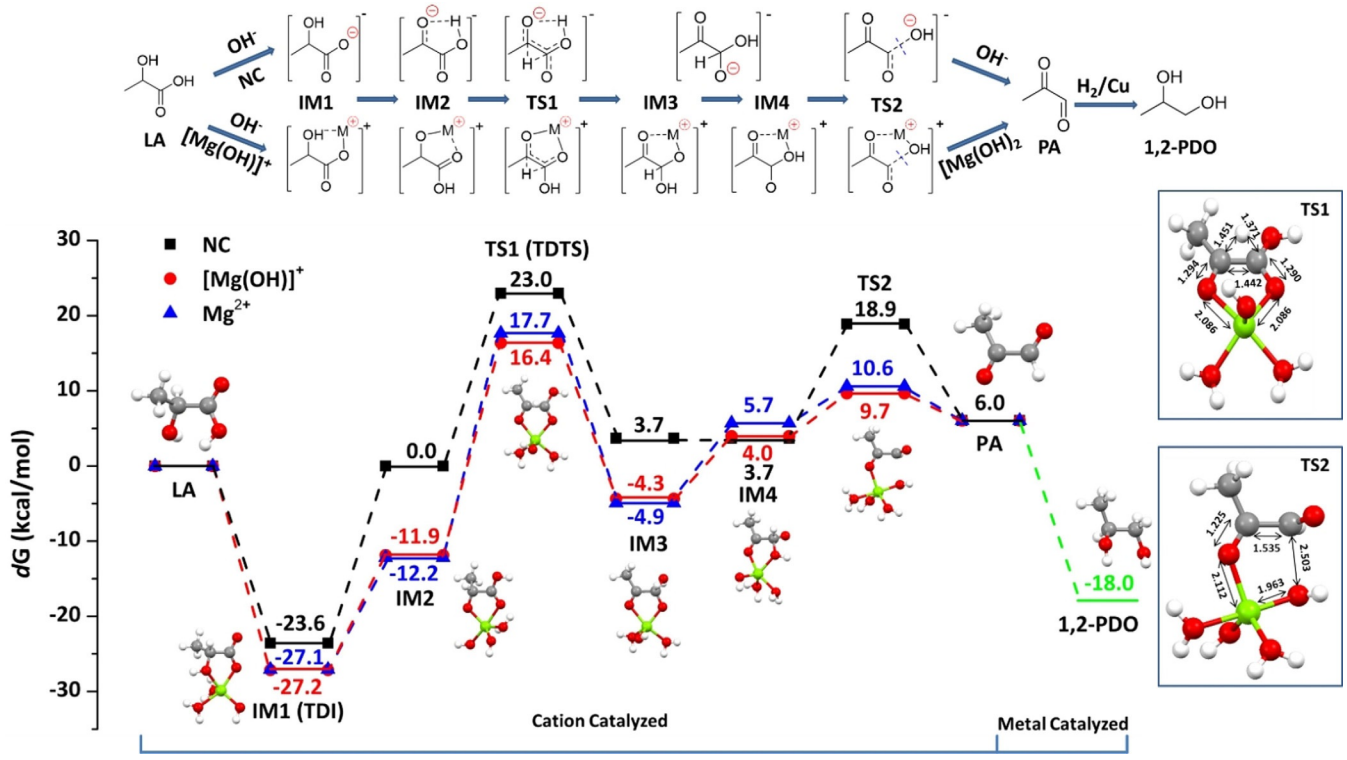


Figure 4. Energy profiles for the conversion of LA into 1,2-PDO in the presence of base conditions (OH^-) with no cation (NC), $[Mg(LA)]^+$ and Mg^{2+} coupled with metal catalyst. Gibbs free energy values are calculated in water and given in kcal mol^{-1}. All atomic distances are given in Å (SMD/B3LYP-D3/6-311++G**); H (white), C (grey), O (red) and Mg (green). TDI and TDTS represent TOF-determining intermediate and TOF-determining transition state.

© 2020 The Authors. Published by Wiley-VCH Verlag GmbH & Co. KGaA, Weinheim

For path NC, elimination of OH^-, going through **TS2** and yielding pyruvaldehyde (PA), can proceed directly. In contrast, for the Mg-ion paths, a proton transfer from one hydroxy group of the gem-diol to the Mg-bound hydroxy (**IM4**) occurs before elimination of OH^- (via **TS2**). As such the base is regenerated at the end of the reaction, which is in accordance with our observations. Finally, PA is hydrogenated over Cu to give 1,2-PDO.

To evaluate the catalytic efficiency of each route, the energetic span (δE) model, which corresponds to the apparent activation energy of the entire catalytic cycle, is applied.[13] Generally, δE is determined based on the TOF-determining transition state (TDTS) and TOF-determining intermediate (TDI). As it has the lowest *d*G among all investigated species, **IM1** is assigned to the TDI. As the *d*G of **TS1** is higher than that of **TS2**, **TS1** is assigned to TDTS. Moreover, the TDI appears before the TDTS, and δE is determined by $dG_{TS1}-dG_{IM1}$. As such, the δE for the NC, $[Mg(OH)]^+$-, and Mg^{2+}-facilitated catalytic routes are 46.6, 43.6, and 44.8 kcal mol^{-1}, respectively. Although δE values of $[Mg(OH)]^+$ and Mg^{2+} are different, both are significantly lower than that of NC.

The Gibbs energy profiles of the conversion of LA into 1,2-PDO involving the rate-determining states in the presence of NC, Ca^{2+} and Mg^{2+} are shown in Figure 5. The *d*G of TDI and TDTS for Ca^{2+} are −25.5 and 21.4 kcal mol^{-1}, respectively. The $\delta E(Ca^{2+})$ is comparable with δE(NC), and 2.1 kcal mol^{-1} higher than $\delta E(Mg^{2+})$. Therefore, the obtained DFT result is in well accordance with the experimental observations that $Mg(OH)_2$ facilitates significantly the conversion of LA in water.

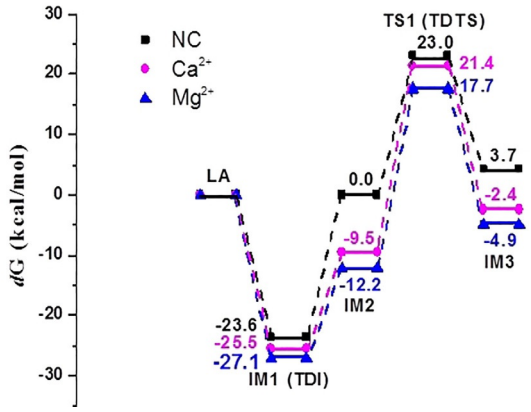


Figure 5. Energy profiles for the conversion of LA into 1,2-PDO involving rate-determining states in the presence of NC, Ca^{2+}, and Mg^{2+}. Gibbs free energy values are calculated in water and given in kcal mol^{-1}.

In summary, we have shown that the liquid-phase conversion of LA into 1,2-PDO can be efficiently achieved with promising yield by using a Cu catalyst in the presence of base. Among various bases, $Mg(OH)_2$ was the most active. $Mg(LA)_2$ was experimentally identified as the key intermediate. DFT calculations demonstrated that the δE value of the reaction in the presence of Mg cations is decreased by 3 kcal mol^{-1} compared to that without cations, confirming the facilitating effect. This combined study provides a promising direction to take advantage of the side product LA in biomass conversion into glycols and deeper insights into this new route.

Acknowledgements

This work was supported by the Cluster of Excellence Fuel Science Center (EXC 2186) financed by the Excellence Initiative of the German federal and state governments to promote science and research at German universities. The authors kindly acknowledge Heike Fickers-Boltz, Elke Biener, and Hannelore Eschmann for the GC analyses, Noah Avraham, Simon Petring for HPLC analyses, Karl Josef Vaeßen for XRD measurement, Heike Bergstein for ICP-OES analyses, and Yongchao Wang and Jingnan Wu for experimental support. X.W. acknowledges a scholarship from the Chinese Scholarship Council.

Conflict of interest

The authors declare no conflict of interest.

Keywords: alcohols · carboxylic acids · copper · hydrogenolysis · magnesium

[1] M. A. Abdel-Rahman, K. Sonomoto, *J. Biotechnol.* **2016**, *236*, 176 – 192.
[2] M. A. Abdel-Rahman, Y. Tashiro, K. Sonomoto, *Biotechnol. Adv.* **2013**, *31*, 877 – 902.
[3] A. M. Ruppert, K. Weinberg, R. Palkovits, *Angew. Chem. Int. Ed.* **2012**, *51*, 2564 – 2601; *Angew. Chem.* **2012**, *124*, 2614 – 2654.
[4] a) I. Delidovich, P. J. C. Hausoul, L. Deng, R. Pfutzenreuter, M. Rose, R. Palkovits, *Chem. Rev.* **2016**, *116*, 1540 – 1599; b) S. J. Tauster, *Acc. Chem. Res.* **1987**, *20*, 389 – 394.
[5] a) K. Tajvidi, P. J. C. Hausoul, R. Palkovits, *ChemSusChem* **2014**, *7*, 1311 – 1317; b) A. K. Beine, A. J. D. Kruger, J. Artz, C. Weidenthaler, C. Glotzbach, P. J. C. Hausoul, R. Palkovits, *Green Chem.* **2018**, *20*, 1316 – 1322; c) R. Y. Sun, M. Y. Zheng, J. F. Pang, X. Liu, J. H. Wang, X. L. Pan, A. Q. Wang, X. D. Wang, T. Zhang, *ACS Catal.* **2016**, *6*, 191 – 201; d) N. Ji, T. Zhang, M. Zheng, A. Wang, H. Wang, X. Wang, J. G. Chen, *Angew. Chem. Int. Ed.* **2008**, *47*, 8510 – 8513; *Angew. Chem.* **2008**, *120*, 8638 – 8641; e) Y. Liu, C. Luo, H. C. Liu, *Angew. Chem. Int. Ed.* **2012**, *51*, 3249 – 3253; *Angew. Chem.* **2012**, *124*, 3303 – 3307; f) X. Wang, A. K. Beine, R. Palkovits, *Stud. Surf. Sci. Catal.* **2019**, *178*, 173 – 193.
[6] H. S. Broadbent, C. W. Whittle, *J. Am. Chem. Soc.* **1959**, *81*, 3587 – 3589.
[7] Z. G. Zhang, J. E. Jackson, D. J. Miller, *Appl. Catal. A* **2001**, *219*, 89 – 98.
[8] Y. Takeda, T. Shoji, H. Watanabe, M. Tamura, Y. Nakagawa, K. Okumura, K. Tomishige, *ChemSusChem* **2015**, *8*, 1170 – 1178.
[9] a) P. J. C. Hausoul, A. K. Beine, L. Neghadar, R. Palkovits, *Catal. Sci. Technol.* **2017**, *7*, 56 – 63; b) P. J. C. Hausoul, L. Negahdar, K. Schute, R. Palkovits, *ChemSusChem* **2015**, *8*, 3323 – 3330; c) H. Adkins, H. R. Billica, *J. Am. Chem. Soc.* **1948**, *70*, 3118 – 3120; d) M. Besson, P. Gallezot, C. Pinel, *Chem. Rev.* **2014**, *114*, 1827 – 1870; e) P. Gallezot, *Chem. Soc. Rev.* **2012**, *41*, 1538 – 1558; f) J. L. Gong, H. R. Yue, Y. J. Zhao, S. Zhao, L. Zhao, J. Lv, S. P. Wang, X. B. Ma, *J. Am. Chem. Soc.* **2012**, *134*, 13922 – 13925; g) R. D. Cortright, M. Sanchez-Castillo, J. A. Dumesic, *Appl. Catal. B* **2002**, *39*, 353 – 359; h) K. T. Liu, X. M. Huang, E. A. Pidko, E. J. M. Hensen, *ChemCatChem* **2018**, *10*, 810 – 817; i) S. Iqbal, S. A. Kondrat, D. R. Jones, D. C. Schoenmakers, J. K. Edwards, L. Lu, B. R. Yeo, P. P. Wells, E. K. Gibson, D. J. Morgan, C. J. Kiely, G. J. Hutchings, *ACS Catal.* **2015**, *5*, 5047 – 5059.
[10] X. Wang, A. K. Beine, P. J. C. Hausoul, R. Palkovits, *ChemCatChem* DOI: https://doi.org/10.1002/cctc.201900299.
[11] M. Valiev, E. J. Bylaska, N. Govind, K. Kowalski, T. P. Straatsma, H. J. J. Van Dam, D. Wang, J. Nieplocha, E. Apra, T. L. Windus, W. de Jong, *Comput. Phys. Commun.* **2010**, *181*, 1477 – 1489.

 © 2020 The Authors. Published by Wiley-VCH Verlag GmbH & Co. KGaA, Weinheim

[12] a) R. Y. Sun, T. T. Wang, M. Y. Zheng, W. Q. Deng, J. F. Pang, A. Q. Wang, X. D. Wang, T. Zhang, *ACS Catal.* **2015**, *5*, 874 – 883; b) Y. L. Wang, W. P. Deng, B. J. Wang, Q. H. Zhang, X. Y. Wan, Z. C. Tang, Y. Wang, C. Zhu, Z. X. Cao, G. C. Wang, H. L. Wan, *Nat. Commun.* **2013**, *4*, 2141; c) D. Rutkowska-Zbik, M. Witko, L. Fiedor, *J. Mol. Model.* **2013**, *19*, 4661 – 4667.

[13] S. Kozuch, S. Shaik, *Acc. Chem. Res.* **2011**, *44*, 101 – 110.

Manuscript received: August 27, 2019
Revised manuscript received: October 1, 2019
Accepted manuscript online: October 8, 2019
Version of record online: October 21, 2019

 © 2020 The Authors. Published by Wiley-VCH Verlag GmbH & Co. KGaA, Weinheim